Improving food value chain through sustainability scores

Hindawi Publishing Corporation
International Journal of Antennas and Propagation
Volume 2012, Article ID 541354, 10 pages
doi:10.1155/2012/541354

Research Article

Neural Network Characterization of Reflectarray Antennas

Angelo Freni,[1] Marco Mussetta,[2] and Paola Pirinoli[3]

[1] *Dipartimento di Elettronica e Telecomunicazioni, Università degli Studi di Firenze, 50121 Florence, Italy*
[2] *Dipartimento di Energia, Politecnico di Milano, 20156 Milan, Italy*
[3] *Dipartimento di Elettronica e Telecomunicazioni, Politecnico di Torino, 10129 Turin, Italy*

Correspondence should be addressed to Marco Mussetta, marco.mussetta@polimi.it

Received 3 March 2012; Accepted 11 May 2012

Academic Editor: Sandra Costanzo

An efficient artificial neural network (ANN) approach for the modeling of reflectarray elementary components is introduced to improve the numerical efficiency of the different phases of the antenna design and optimization procedure, without loss in accuracy. The comparison between the results of the analysis of the entire reflectarray designed using the simplified ANN model or adopting a full-wave characterization of the unit cell finally proves the effectiveness of the proposed model.

1. Introduction

Printed reflectarrays (RAs) have become nowadays a well-established technology for the realization of high performance antennas to be used in different applications, ranging from earth stations or onboard antennas in satellite communication systems to radar antennas mounted on vehicles (see e.g., [1–10]).

The need of providing high performances and satisfying potentially conflicting requirements generally forces the use of complex configurations, with a large number of reradiating elements. At their turn, the latter could present a complex structure, with several degrees of freedom, which have to be adjusted in order to satisfy the antenna constraints. All these factors concur to increase the RA design complexity and, therefore, the use of an indirect synthesis procedure based on an optimization algorithm could be convenient, since it can handle a large number of degrees of freedom and provide a configuration satisfying at the best the different constraints on the antenna [11–13].

The RA design procedure can be seen as the cascade of two steps, organized as in the block diagram of Figure 1: the characterization of the single RA reradiating element with respect to several parameters, and the optimized design of the entire structure, managed by a global optimization tool. A further step could be added, before the antenna manufacturing, consisting in a full-wave analysis of the entire RA (virtual prototyping).

The starting point of the design procedure is to obtain a map of the phase and the amplitude of the reflection coefficient of the RA single element as a function of selected geometrical parameters. This is usually done adopting a full wave MoM approach and considering the single RA element embedded in a periodic lattice on which a plane wave impinges. The generation of these maps is computationally expensive, since it requires the full-wave analysis of the periodic array for several values of the free geometrical parameters, as well as for different frequencies and angles of incidence. Moreover, if the design of the entire reflectarray is carried out exploiting an optimization procedure, based on the use of a pseudo-stochastic algorithm, the reflection coefficient sampling rate has to be quite high. Finally, the storage of data produced by these simulations requires a large amount of dynamic memory. In view of reducing these computational and memory efforts, it would be useful to introduce an equivalent model of the reradiating element. If its geometry is simple, its behavior could be approximated with an equivalent transmission line model [11, 14]: in this case, no full-wave analysis has to be carried out, since the simplified model is directly managed by the optimization tool. Unfortunately, such an approximation is no longer applicable when the geometry complexity increases and a more general model is required.

Here, a modeling technique, independent from the RA reradiating element structure and able to reproduce its

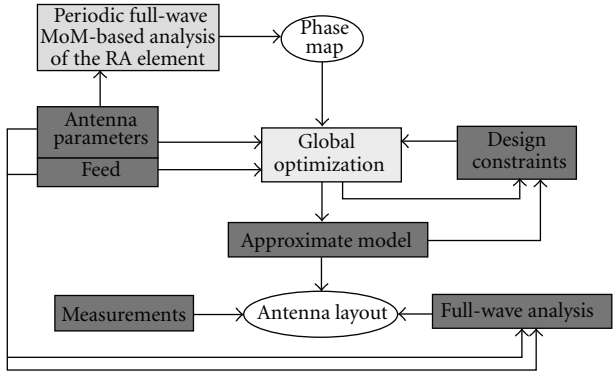

Figure 1: Block diagram of the proposed design procedure.

behavior at a reduced computational cost, is presented. It is based on the use of an artificial neural network (ANN) for simulating the relationship between the local re-radiated field and the geometrical parameters of the element, so that it becomes possible to compute the reflection coefficient of the reradiating element for any value of the RA parameters, starting from a reduced set of data obtained through the standard full-wave analysis.

Preliminary results of the modeling of a RA reradiating element behavior with an ANN have been presented in [15], where only some plots of the phase of the reflection coefficient computed with the ANN and a guess of the introduced error are shown, and in [16] where the reflection coefficient phase reconstructed by the ANN has been used to compute the field re-radiated by a reflectarray in which the reradiating elements are double square concentric rings and only one geometric parameter has been used to control the phase variation. The validity of the approach has been confirmed also in [17], where it is used for the reflection coefficient phase of a multilayer reradiating element; however, also in this paper only the results about the comparison between the full-wave and the ANN computed reflection coefficient are shown.

Here, the ANN model will be used for computing the variation of the *entire* reflection coefficient for both the vertical and horizontal polarizations with the reradiating element geometrical parameters, the frequency, and the angle of incidence. First, the computational time and the memory reduction due to the introduction of the ANN are investigated, considering reradiating elements of increasing complexity. Then, the attention has been focused on the RA introduced in [7] where the reradiating elements are modified Malta Cross, characterized by two geometrical degrees of freedom for controlling the re-radiated field: the effect of the use of the ANN model will be considered not only analyzing the error introduced on the reflection coefficient, but also that on the field radiated by the entire reflectarray.

2. Artificial Neural Networks

An artificial neural network (ANN) is a computational model that simulates the features and behaviors of the human brain neurons [18, 19], that is, it is a self-adaptive data modeling tool that changes its structure on the basis of external or internal information that flows through the network during the learning phase. In particular, an ANN consists of an interconnected group of artificial neurons that suitably processes information according to the strength of connections among them.

In more practical terms neural networks are nonlinear statistical data modeling tools. They can be used to model complex relationships between inputs and outputs or to find patterns in data. For this reason, ANNs are useful tools when it is necessary to understand the complex and nonlinear relationships among data, without any a priori assumption concerning the nature of these correlations.

In recent years, ANN have been extensively employed in many antenna applications and in particular in problems involving smart antennas: in [20] an ANN is employed to model the active-aperture antenna shape in real time, in [21, 22] direction-of-arrival and multiple-source tracking for wireless terrestrial, and satellite mobile communications are addressed employing neural-network-based smart antennas. Moreover, in [23] ANNs are applied to the scattering of a nonlinearly loaded antenna by modeling its RCS. ANN has been also used for antenna optimization in conjunction with evolutionary algorithms: in [24] the design of a wideband microstrip antenna is performed using a genetic-algorithm-coupled ANN in computing the radiation pattern and the resonant frequency; in [25] an ANN is proposed to predict the input impedance of a broadband antenna as a function of its geometric parameters. The antenna structure is then optimized for broadband operation via a genetic algorithm that uses input impedance estimates provided by the trained ANN. Patch antenna modeling is another application of ANN: in [26] an ANN is used to design the parameters of square and rectangular patch antenna; in [27] a neural network model of slotted patch antenna is developed to calculate the resonant frequency and minimum value of S_{11} parameter considering both antenna dimensions and dielectric characteristics. Moreover, in [28] a neural network-based solution is employed to relate a given radiated field distribution with the voltages that must be applied to each radiating element taking into account mutual coupling effects without increase of complexity.

The characteristics of an ANN depend on its topology, that is, on the pattern of connections between the neurons and the propagation of data. Here, for the modeling of the reradiating element behavior, the multilayered perceptron (MLP), has been used.

The MLP implements a feed-forward topology, in which the data flow from the input to the output layers is strictly forward, and consists of an input layer, one or more hidden layer, and an output layer. The resulting network structure is that depicted in Figure 2, where the dependencies between variables are represented by the connections among neurons. The input composition in each neuron is made by a nonlinear weighted sum,

$$f(x) = k(x)\left(\sum_i w_i g_i(x)\right), \tag{1}$$

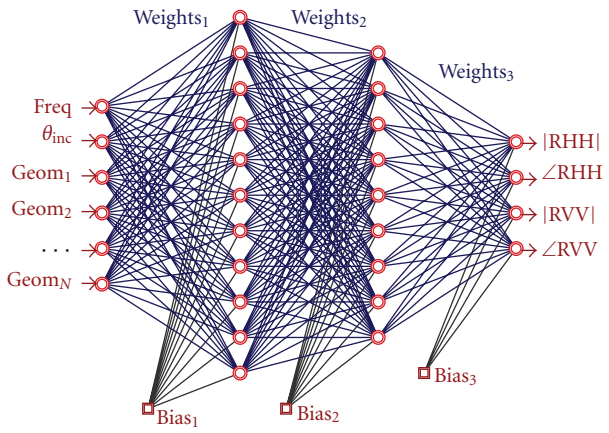

Figure 2: A typical multilayered perceptron structure, with 6 input and 4 output neurons and 2 hidden layers of 11 and 9 neurons, respectively.

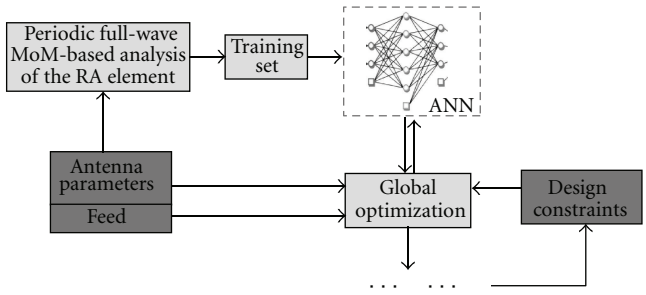

Figure 3: Part of the block diagram of Figure 1 modified by introduction of ANN.

where $k(x)$ is a nonlinear activation function which models the activity of biological neurons in the brain. This function must always be normalizable and differentiable and it is modeled in several ways; the most common is the hyperbolic tangent, which ranges from -1 to 1:

$$k(x) = \tanh(x). \tag{2}$$

2.1. Neural Network Training. A neural network works properly when, for any set of inputs, it produces the desired set of outputs. This means that the connections between the different nodes in the network are set properly, that is, the weights w_i have been correctly chosen.

The definition of these weights is generally done during a training phase: in the so-called *supervised learning* scheme the neural network is fed with a set of input-output pairs already known, called Training Set (TS): for a given number N of these pairs (x_i, y_i), where $x_i \in X$, $y_i \in Y$, it is necessary to find a function:

$$f : X \longrightarrow Y, \tag{3}$$

that matches the examples of the TS. Thus, weights are changed according to a suitable learning rule, until the error on the ANN outputs is minimized [29].

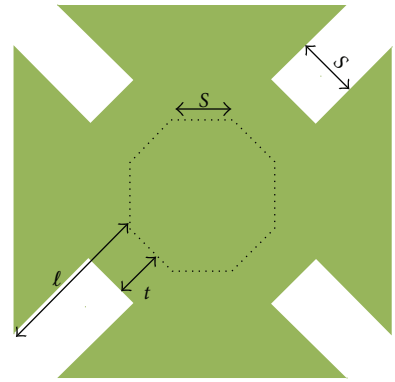

Figure 4: Single cell of the modified Malta Cross.

Among different learning rules, error backpropagation (EBP) is a well-known analytical algorithm used for neural networks training. In literature, there are several forms of backpropagation, all of them requiring different levels of computational efforts; the conventional back-propagation method is, however, the one based on the gradient descent algorithm. EBP propagates error backwards through the network to allow the error derivatives for all network weights to be efficiently computed. In other words, network weights are optimized in order to reach a good and accurate output and this objective is reached typically minimizing the mean-squared error between the network's output, $f(x_i)$, and the target value y_i over all the N example pairs.

Training is time and memory consuming and is the most critical phase in the ANN set up, since it must provide continuous feedback on the quality of solutions obtained thus far.

To test the ANN generalization capability, a validation set (VS) is defined too, containing known (x_i, y_i) pairs not used in the TS, in order to check the correct association between unknown input and output data.

2.2. Neural Network Use in RA Characterization. Once trained, the ANN can be considered as a black box: the desired output can be forecast for any arbitrary set of input data. For the case under analysis, the inputs are represented, as sketched in Figure 2, by the reradiating element geometrical degrees of freedom, the frequency, and the angle of incidence, while the expected output is the total reflection coefficient for both the horizontal and vertical polarization. Note that the angle of incidence of the impinging field could noticeably vary from one border to the other of the planar reflector, especially when it has a large electrical size and the feed is offset. Note also that generally the amplitude of the reflection coefficient is neglected during the design of a RA, since it is assumed to be equal to unity; however, for some particular values of the geometrical parameters, this amplitude decreases (at the structure resonances), and therefore it becomes necessary to take into account also of this phenomenon.

It has been found that the relation between the above inputs and outputs could properly model with an ANN

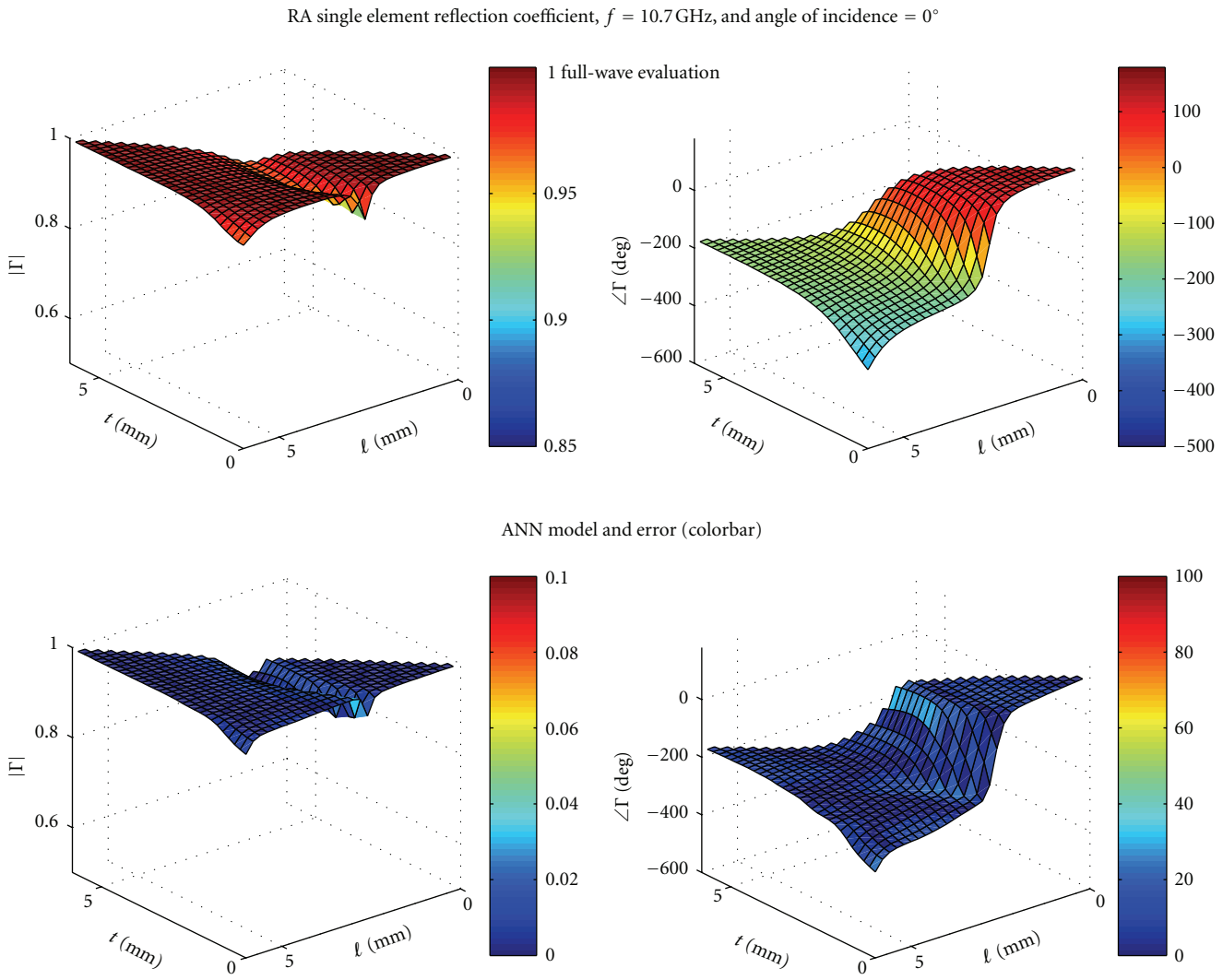

FIGURE 5: Reflection coefficient amplitude (left) and phase (bottom) versus the two RA geometrical parameters ℓ and t of the modified Malta Cross, computed with direct full-wave (top) and reconstructed with the ANN (bottom). $f = 10.7$ GHz, $\theta_{inc} = 0°$.

consisting in two hidden layers with 11 neurons in the first layer and 9 in the second one.

Introducing the ANN model of the reradiating element, the RA design procedure is modified as sketched in Figure 3, with the advantage that only the TS data are computed with the full wave approach and stored only for the training phase, since after that they are useless. In fact, during the RA design procedure, guided by the optimization tool, this latter will directly introduce in the ANN the geometrical free parameters relative to each RA element and the ANN will produce the corresponding reflection coefficient, with a clear reduction of the computational time and of the memory requirements, as proved by the results relative to different types of reradiating elements reported in the next section.

3. Numerical Results

The effectiveness of the use of a proper ANN for modeling the behavior of a single RA element has been investigated, considering both its numerical efficiency and the error introduced not only on the single element reflection coefficient, but also on the radiation patterns of an entire RA.

For what concerns the ANN model numerical efficiency, we have considered different types of reradiating elements, with different degrees of complexity, and for all of them we have computed the time and the memory reduction introduced by the ANN model. For doing that, first we have computed the reflection coefficient maps with the periodic full-wave approach; since they depend also on both the frequency and the angle of incidence, which, at their turn, vary from one application to another, we have decided to refer, as a reference example, to a particular reflectarray, the one that is described in [7]: it consists of 36×36 elements, corresponding to an electrical size of almost $16\lambda \times 16\lambda$ at the central frequency of 11.7 GHz, it is offset fed, and the direction of maximum radiation forms a slant angle of 15° with respect to the broadside. Moreover, the design has been carried out so that the antenna works on the frequency band

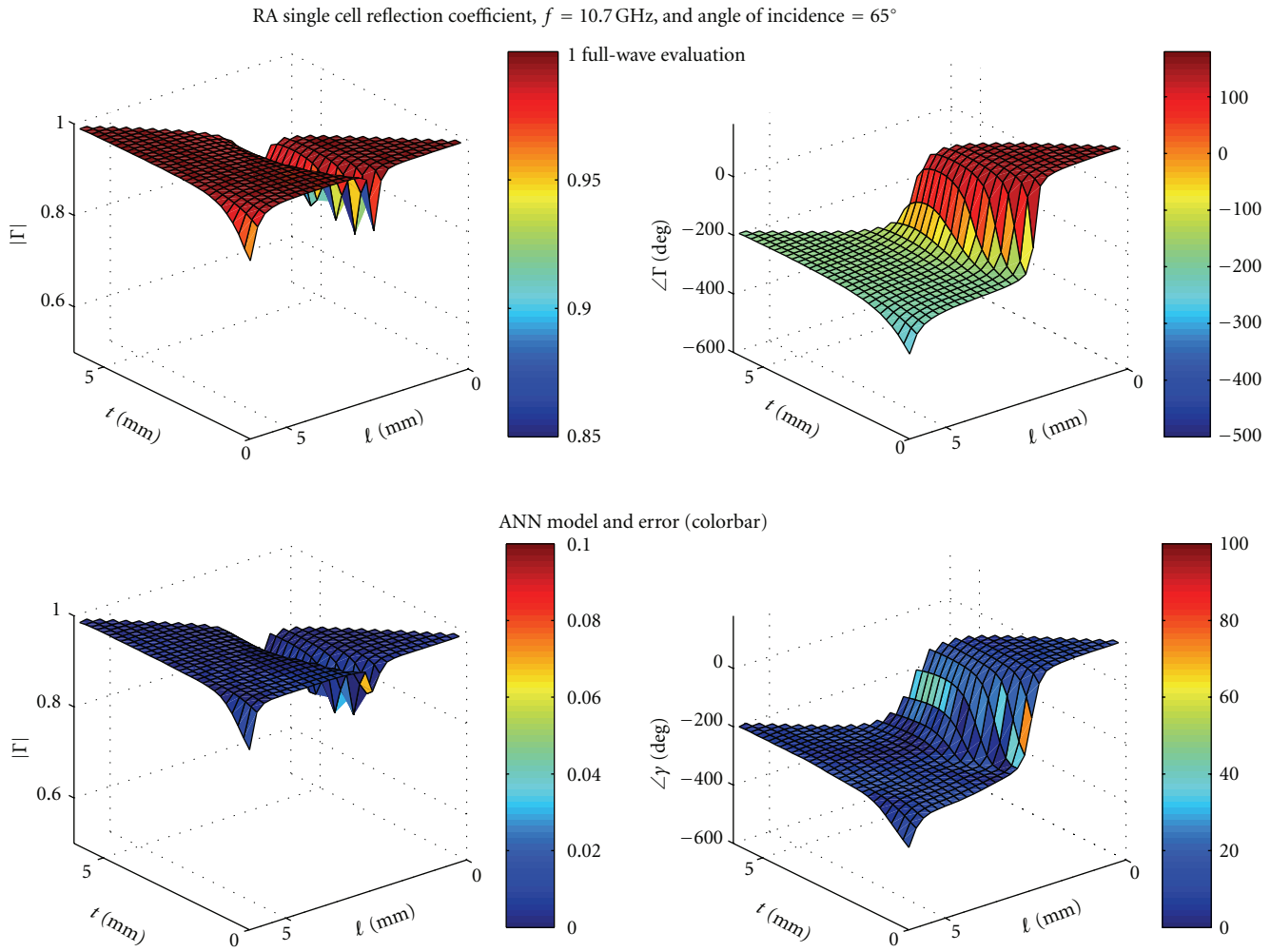

FIGURE 6: Reflection coefficient amplitude (left) and phase (bottom) versus the two RA geometrical parameters ℓ and t of the modified Malta Cross, computed with direct full-wave (top) and reconstructed with the ANN (bottom). f = 10.7 GHz, $\theta_{\text{inc}} = 65°$.

[10.7–12.7] GHz. For such a structure, it has been seen that a total number of 50 samples is required to well represent the reflection coefficient variation with frequency and angle of incidence. Note that the maximum angle of incidence considered is equal to 65° and that the variation of the reflection coefficient increases for greater angle of incidence. This behaviour makes it necessary to consider a not uniform sampling of this quantity. This number of frequency and angle of incidence samples will be assumed to be the same for all the different types of reradiating element that will be considered in the following.

The simplest type of reradiating element we have considered has been a square, single-layer patch, for which the reflection coefficient variation is obtained varying the side ℓ of the patch itself. It has been seen that a reasonable discretization of the interval of variation for ℓ is obtained with 35 samples. As a second example of reradiating element, we have considered the modified Malta Cross introduced in [7] and shown also in Figure 4 for the sake of clarity, in which, to better control the frequency dependence of the re-radiated field and to enhance the bandwidth, two geometrical parameters, that is, ℓ and t in Figure 4, are used. Their good discretization is reached with 31 samples for each of the two geometrical quantities. The other two configurations considered consist in two and three-layer stacked square patches. In both cases the geometrical free parameters are the side of the square patches, whose interval of variation has been discretized with 34 samples each.

In the second and third columns of Table 1, it is reported the total time needed to compute the reflection coefficient maps and the dynamic memory necessary for their storage using the periodic full-wave approach relatively to the four types of reradiating elements. These full-wave simulations have been performed using Ansoft Designer, on an Intel Core2 Duo E4700, 2.6 GHz, 2 Gb RAM system. Note that both the computational cost and the memory requirements increase drastically with the reradiating element complexity.

In view of reducing both the computational time and the memory occupation, the dependence of the reflection coefficient from the free geometrical parameters of each reradiating element, from the frequency, and from the angle

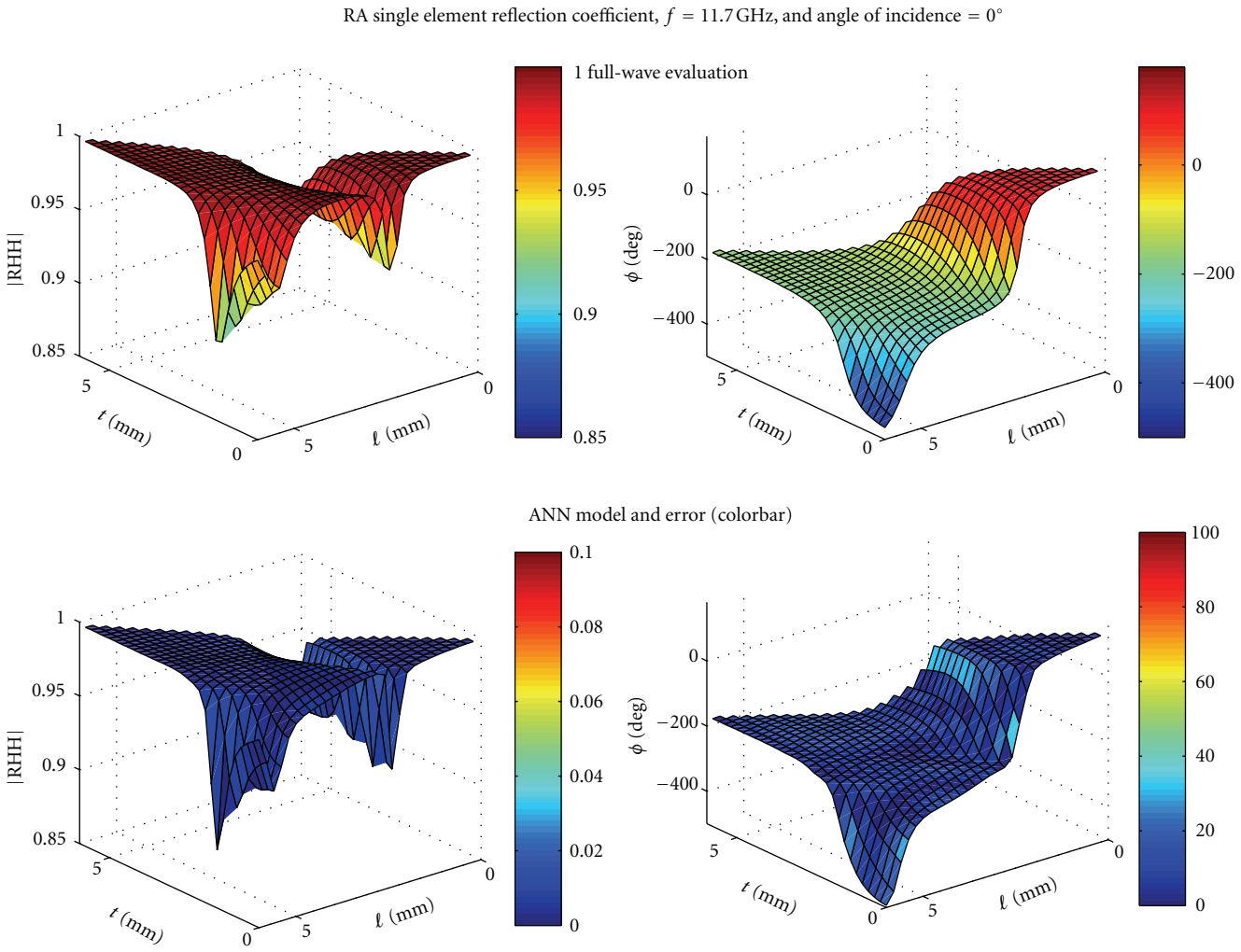

Figure 7: Reflection coefficient amplitude (left) and phase (bottom) versus the two RA geometrical parameters ℓ and t of the modified Malta Cross, computed with direct full-wave (top) and reconstructed with the ANN (bottom). f = 11.7 GHz, $\theta_{\text{inc}} = 0°$.

Table 1: Computational time and memory requirement for the evaluation and the storage of the reflection coefficient maps for different types of re-radiating elements, with the periodic full-wave approach and the ANN training.

Element type	Full wave		ANN training	
	Computational time	Memory requirement	Computational time	Memory requirement
1-layer square patch	4 h 45 min	0.9 Mb	55 min	9.5 Kb
1-layer modified Malta Cross	65 h	2.5 Mb	4 h	134 Kb
2-layer stacked patches	241 h	3.2 Mb	13 h 30 min	160 Kb
3-layer square patches	1.2×10^4 h	67 Mb	341 h 50 min	2.87 Mb

of incidence has been modeled with the ANN described in Section 2.

Since the most critical end expensive phase in the use of an ANN is its training, we consider here as the ANN computational cost and memory occupation those required in that phase. The computational time required for the neural network training is given by the sum of the time necessary to compute the data for the training and that required by the actual training. In the fourth column of Table 1 the training total computational time for the four reradiating element is reported. The data for the training are still obtained with the full-wave simulations: it has been seen that a good reconstruction of the reflection coefficient has been guaranteed by 10 samples for the total of frequency and angle of incidence, while the number of samples for the geometrical parameters varies from one element to another. Comparing the second and the fourth columns of Table 1, it is possible to see that the ANN training requires globally a computational cost varying from 0.19 to 0.028 times that needed for collecting the data when the traditional approach

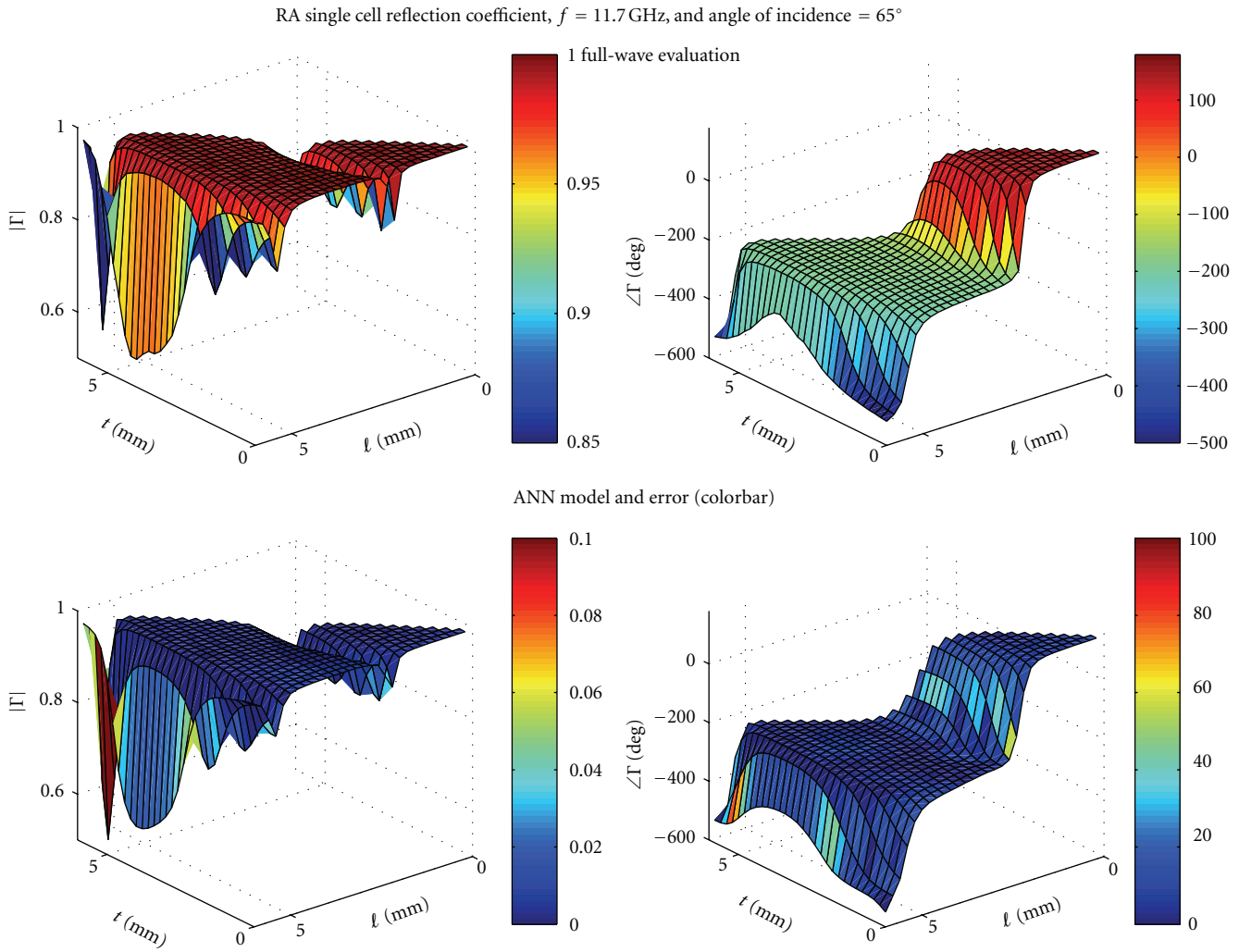

FIGURE 8: Reflection coefficient amplitude (left) and phase (bottom) versus the two RA geometrical parameters ℓ and t of the modified Malta Cross, computed with direct full-wave (top) and reconstructed with the ANN (bottom). f = 11.7 GHz, $\theta_{inc} = 65°$.

is used. Note that, when used in the RA design and/or analysis procedure, the computational time required by the ANN to compute the reflection coefficient in correspondence of a value for the geometrical degrees of freedom, for the frequency and for the angle of incidence is of the order of 40 μsec.

The use of the neural network drastically reduces also the memory occupation: in the fifth column of Table 1, it is reported the dynamic memory needed to store the data during the training section, obviously lower than the case in which the full-wave approach is used. However, it has to be remarked that the memory reduction factor, that comes out from comparing the third and the fifth column of Table 1, is valid only for the training section, since at the end of the training these data could be removed, and the memory occupation of the neural network is around 5 KB, equal to 0.002 times that required by collecting all the data used in the traditional approach.

In order to verify if the use of the ANN for the modeling of the RA single cell does not only guarantees a strong reduction of both the computational cost and of the memory requirement but also gives its accurate representation, we have also investigated the error that ANN model introduces on the reflection coefficient and on the radiating characteristics of the RA. With this aim, we have considered the 16×16 offset reflectarray already introduced in [7] and described at the beginning of this section, in which the reradiating elements are the modified Malta Cross.

Figures 5, 6, 7, and 8 show the variation of the reflection coefficient phase and amplitude with the two geometrical parameters ℓ and t reconstructed using the ANN (bottom) or obtained by the direct full-wave analysis of the periodic structure (top), for one of the extremes and the central frequency of the RA band and for two different angles of incidence ($\theta_{inc} = 0°$ and $\theta_{inc} = 65°$). The colorbars on the top give the values of the reflection coefficient amplitude (left) and phase (right), while those on the bottom show the error introduced by the use of the ANN model.

From the plots in Figures 5, 6, 7, and 8, it is possible to draw the following conclusions:

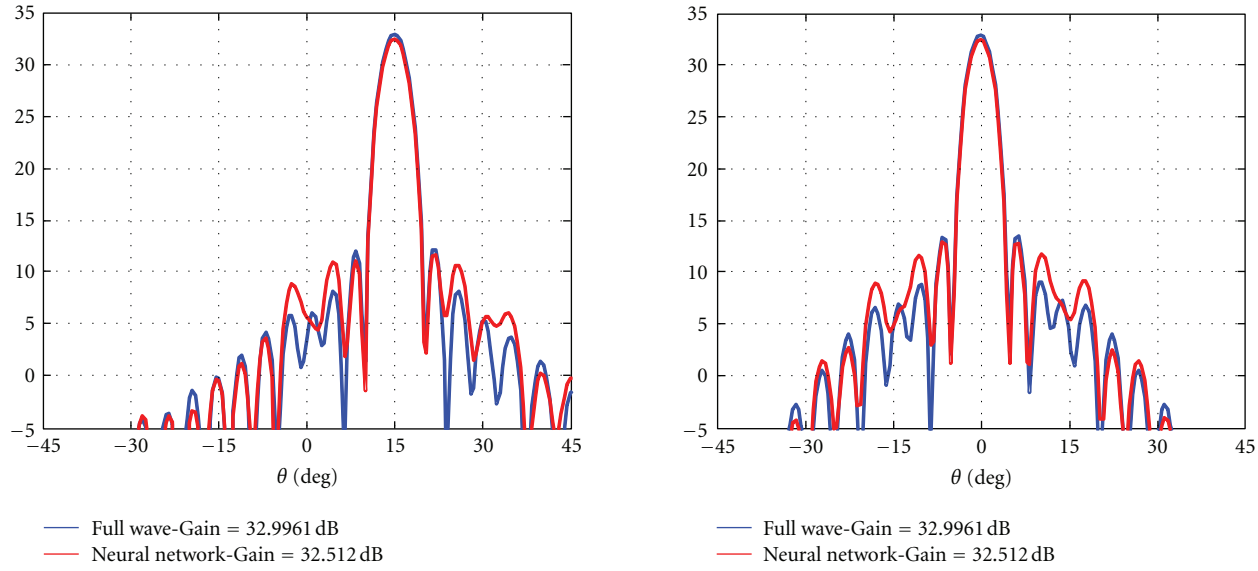

Figure 9: Radiation pattern of the RA antenna with modified Malta Cross reradiating elements at 7.8 GHz: comparison between the results obtained using full-wave computed reflection coefficient values or ANN.

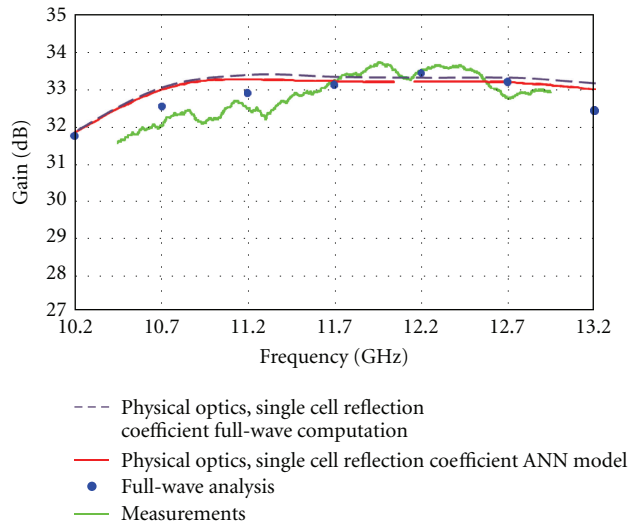

Figure 10: Variation of the maximum gain on the band 10.7–12.7 GHz for the RA with modified Malta Cross reradiating elements.

(i) the amplitude of the reflection coefficient does not vary substantially for low values of frequency and angles of incidence;

(ii) the error introduced by the ANN on the amplitude of the reflection coefficient is really small;

(iii) the phase varies in the range [0–600°];

(iv) the error introduced by the use of the ANN on the phase is well controlled, even if there are some single spots, where the slope of the phase curve is higher than could become remarkable. It is worth noting that these spots take place in correspondence of the RA element resonances where the full-wave analysis is critical. However, this error is really localized and it will not affect the computation of the RA radiation parameters.

The ANN model of the single reradiating element has then be used in computing the gain pattern of the entire RA by using the physical optics approximation. Figure 9 shows the antenna gain patterns at the central frequency of 11.7 GHz for both the principal planes. The gain patterns have been computed by using both the exact value and the ANN approximation of the reflection coefficient. The relevant plots show a good agreement: the main beams are almost coincident and also the relative error introduced by the ANN on the sidelobes is always below few percent.

A similar observation applies also to the plot in Figure 10, in which the variation of the maximum gain versus frequency, computed with different techniques or obtained from the measurement of a prototype of the designed antenna, is shown. In particular, when we compare the results obtained by using the physical optics approximation together with the data for the reflection coefficient computed through the full-wave simulation of the unit cell (dash line) or by adopting the ANN approximated model (continuous line), it is evident that the latter underestimates the antenna gain. However, if we look at the values obtained by applying the MoM to the entire antenna [30] (dots) and the measurement results, it is evident that the error introduced by the ANN approximated model is negligible with respect to the one introduced by the physical optics approximation itself. Thus, the ANN approximated model can be conveniently used to obtain a reflectarray layout and to make a first optimization of the RA with the same uncertainty of the time-consuming accurate interpolation of the reflection coefficients.

4. Conclusions

The results of the previous section confirm the validity of the proposed characterization technique for the modeling of the behaviour of the RA reradiating element. The use of the artificial neural network for the characterization of the relationship between the RA single element reflection coefficient and the geometrical parameters that affect it allows a drastic reduction of both the computational time and the memory storage, without altering the accuracy of the solution.

References

[1] J. Huang and J. A. Encinar, *Reflectarray Antennas*, Wiley-IEEE Press, 2007.

[2] J. A. Encinar and J. A. Zornoza, "Broadband design of three-layer printed reflectarrays," *IEEE Transactions on Antennas and Propagation*, vol. 51, no. 7, pp. 1662–1664, 2003.

[3] D. Cadoret, A. Laisné, R. Gillard, L. Le Coq, and H. Legay, "Design and measurement of new reflectarray antenna using microstrip patches loaded with slot," *Electronics Letters*, vol. 41, no. 11, pp. 623–624, 2005.

[4] J. A. Encinar, L. Datashvili, J. A. Zornoza et al., "Dual-polarization dual-coverage reflectarray for space applications," *IEEE Transactions on Antennas and Propagation*, vol. 54, no. 10, pp. 2827–2837, 2006.

[5] S. Costanzo, F. Venneri, and G. Di Massa, "Bandwidth enhancement of aperture-coupled reflectarrays," *Electronics Letters*, vol. 42, no. 23, pp. 1320–1322, 2006.

[6] Z. H. Wu, W. X. Zhang, Z. G. Liu, and W. Shen, "A dual-layered wideband microstrip reflectarray antenna with variable polarization," *Microwave & Optical Technology Letters*, vol. 48, no. 7, pp. 1429–1432, 2006.

[7] P. De Vita, A. Freni, G. L. Dassano, P. Pirinoli, and R. E. Zich, "Broadband element for high-gain single-layer printed reflectarray antenna," *Electronics Letters*, vol. 43, no. 23, pp. 1247–1249, 2007.

[8] P. Pirinoli, P. T. Cong, M. Mussetta, and M. Orefice, "Concentric square ring elements for dual band reflectarray antenna," in *Proceedings of the 3rd European Conference on Antennas and Propagation (EUCAP '09)*, pp. 1342–1344, Berlin, Germany, March 2009.

[9] L. Moustafa, R. Gillard, F. Peris, R. Loison, H. Legay, and E. Girard, "The phoenix cell: a new reflectarray cell with large bandwidth and rebirth capabilities," *IEEE Antennas and Wireless Propagation Letters*, vol. 10, pp. 71–74, 2011.

[10] K. K. Kishor and S. V. Hum, "An amplifying reconfigurable reflectarray antenna," *IEEE Transactions on Antennas and Propagation*, vol. 60, no. 1, pp. 197–205, 2012.

[11] M. Mussetta, G. L. Dassano, P. Pirinoli, R. E. Zich, and M. Orefice, "18 GHz microstrip reflectarray: GA optimization and experimental measurements," in *Proceedings of the Journes Internationales de Nice sur les Antennes*, pp. 240–241, Nice, France, 2004.

[12] I. Barriuso, A. L. Gutiérrez, M. Lanza et al., "Comparison of heuristic methods when applied to the design of reflectarrays," in *Proceedings of the 5th European Conference on Antennas and Propagation (EUCAP '11)*, pp. 970–974, Rome, Italy, April 2011.

[13] Y. Aoki, H. Deguchi, and M. Tsuji, "Reflectarray with arbitrarily-shaped conductive elements optimized by genetic algorithm," in *Proceedings of the IEEE International Symposium on Antennas and Propagation and USNC/URSI National Radio Science Meeting*, pp. 960–963, 2012.

[14] M. Bozzi, S. Germani, and L. Perregrini, "A figure of merit for losses in printed reflectarray elements," *IEEE Antennas and Wireless Propagation Letters*, vol. 3, no. 1, pp. 257–260, 2004.

[15] D. Caputo, A. Pirisi, M. Mussetta, A. Freni, P. Pirinoli, and R. E. Zich, "Neural network characterization of microstrip patches for reflectarray optimization," in *Proceedings of the 3rd European Conference on Antennas and Propagation (EUCAP '09)*, pp. 2520–2522, Berlin, Germany, March 2009.

[16] M. Mussetta, P. Pirinoli, P. T. Cong, M. Orefice, and R. E. Zich, "Optimization of a dual-layer reflectarray antenna by means of soft-computing techniques," in *Proceedings of the 12th International Conference on Electromagnetics in Advanced Applications (ICEAA '10)*, pp. 716–719, September 2010.

[17] P. Robustillo, J. A. Encinar, and J. Zapata, "ANN element characterization for reflectarray antenna optimization," in *Proceedings of the 5th European Conference on Antennas and Propagation (EUCAP '11)*, pp. 957–960, Rome, Italy, April 2011.

[18] Haykin, *Neural Networks: A Comprehensive Foundation*, Prentice-Hall, Upper Saddle River, NJ, USA, 1999.

[19] Q. J. Zhang and K. C. Gupta, *Neural Networks for RF and Microwave Design*, Artech House, Norwood, Mass, USA, 2000.

[20] G. Washington, "Aperture antenna shape prediction by feed-forward neural networks," *IEEE Transactions on Antennas and Propagation*, vol. 45, no. 4, pp. 683–688, 1997.

[21] E. Charpentier and J.-J. Laurin, "An implementation of a direction-finding antenna for mobile communications using a neural network," *IEEE Transactions on Antennas and Propagation*, vol. 47, no. 7, pp. 1152–1159, 1999.

[22] A. H. El Zooghby, C. G. Christodoulou, and M. Georgiopoulos, "A neural network-based smart antenna for multiple source tracking," *IEEE Transactions on Antennas and Propagation*, vol. 48, no. 5, pp. 768–776, 2000.

[23] K. C. Lee, "Application of neural network and its extension of derivative to scattering from a nonlinearly loaded antenna," *IEEE Transactions on Antennas and Propagation*, vol. 55, no. 3, part 2, pp. 990–993, 2007.

[24] D. K. Neog, S. S. Pattnaik, D. C. Panda, S. Devi, B. Khuntia, and M. Dutta, "Design of a wideband microstrip antenna and

the use of artificial neural networks in parameter calculation," *IEEE Antennas and Propagation Magazine*, vol. 47, no. 3, pp. 60–65, 2005.

[25] K. Youngwook, S. Keely, J. Ghosh, and H. Ling, "Application of artificial neural networks to broadband antenna design based on a parametric frequency model," *IEEE Transactions on Antennas and Propagation*, vol. 55, no. 3, part 1, pp. 669–674, 2007.

[26] A. Mishra, A. B. Nandgaonkar, V. D. Bhagile, S. C. Mehrotra, and P. M. Patil, "Design of square and rectangular microstrip antenna with the use of FFBP algorithm of artificial neural network," in *Proceedings of the Applied Electromagnetics Conference (AEMC '09)*, December 2009.

[27] M. Milijić, Z. Stanković, and B. Milovanović, "Efficient model of slotted patch antenna based on neural networks," in *Proceedings of the 9th International Conference on Telecommunications in Modern Satellite, Cable, and Broadcasting Services (TELSIKS '09)*, pp. 384–387, 2009.

[28] R. G. Ayestarán, F. Las-Heras, and L. F. Herrán, "Neural modeling of mutual coupling for antenna array synthesis," *IEEE Transactions on Antennas and Propagation*, vol. 55, no. 3, part 2, pp. 832–840, 2007.

[29] L. Hamm, B. W. Brorsen, and M. T. Hagan, "Global optimization of neural network weights," in *Proceedings of the International Joint Conference on Neural Networks (IJCNN '02)*, pp. 1228–1233, May 2002.

[30] P. De Vita, F. De Vita, A. Di Maria, and A. Freni, "An efficient technique for the analysis of large multilayered printed arrays," *IEEE Antennas and Wireless Propagation Letters*, vol. 8, pp. 104–107, 2009.